THE ACTIVE COUPLING OF ELECTROMAGNETIC WAVES HAVING DIFFERING PHASE CONSTANTS

Albert Edward Whitehead

United States
Naval Postgraduate School

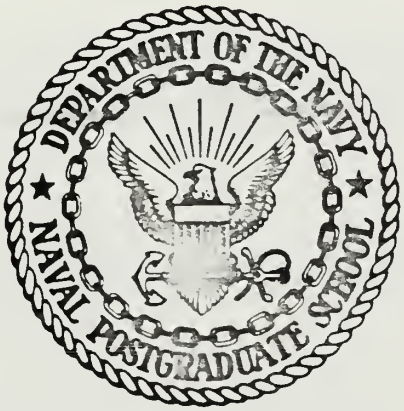

THESIS

THE ACTIVE COUPLING OF ELECTROMAGNETIC WAVES HAVING DIFFERING PHASE CONSTANTS

by

Albert Edward Whitehead

Thesis Advisor: J. B. Knorr

December 1971

Approved for public release; distribution unlimited.

The Active Coupling of Electromagnetic Waves Having Differing Phase Constants

by

Albert Edward Whitehead
Lieutenant, United States Navy
B.S.E.E., University of Idaho, 1964

Submitted in partial fullfillment of the
requirements for the degree of

MASTER OF SCIENCE IN ELECTRICAL ENGINEERING

from the

NAVAL POSTGRADUATE SCHOOL
December 1971

ABSTRACT

The theory of active coupling of two waves with differing phase constants is examined. Experimental results supporting this theory are presented which include coupled power measurements and variations in coupling parameters as a function of the physical structure.

It is pointed out that this investigation could be applied directly to filter design and provides background work for the design of a broadband coupler.

TABLE OF CONTENTS

LIST OF ILLUSTRATIONS

I. INTRODUCTION

A. BACKGROUND OF COUPLED MODE THEORY

1. Transmission Line Equations for Coupled Modes

The theory of coupled modes of propagation, first well formalized by J. R. Pierce [1] in 1954, is now well understood and has been used to explain wave interactions and the operation of many devices. In general it has been applied to interactions between waves with equal phase constants and uniform coupling. More recently proposals have been made that waves with differing phase constants may be coupled by utilizing periodic coupling provided the proper structure period is chosen.

Consider the two arbitrary transmission lines shown in Figure 1 which are uniformly coupled over a distance L.

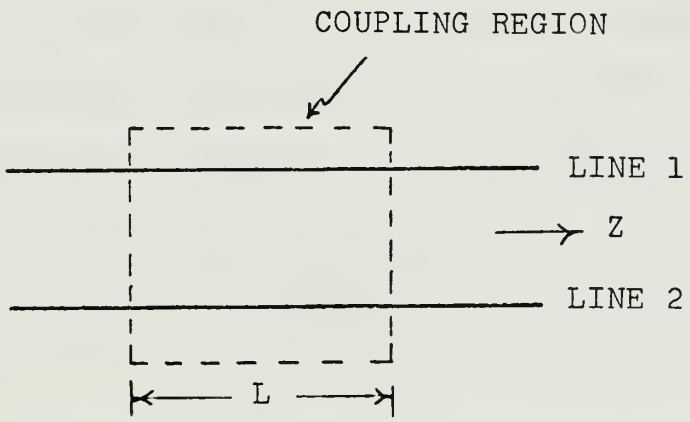

Figure I. Uniformly Coupled Lines.

Classical treatment of this situation requires solution of the coupled line equations (1) and (2)

$$j\frac{\partial A_1}{\partial Z} = \beta_1 A_1 + C_{12}A_2 \tag{1}$$

$$j\frac{\partial A_2}{\partial Z} = C_{21}A_1 + \beta_2 A_2 \tag{2}$$

where β_n = the uncoupled phase constant of the n^{th} line

$C_{m,n}$ = the coupling coefficient between lines m and n

A_n = the wave amplitude on the n^{th} line

It may be shown, [2], that the solution for the coupled phase constants β' is

$$\beta'_{1,2} = \beta_1 + \frac{\Delta\beta}{2} \pm \sqrt{C_{12}C_{21} - \left(\frac{\Delta\beta}{2}\right)^2} \tag{3}$$

and when

$$\Delta\beta = 0,\ \beta'_{1,2} = \beta_1 \pm j\sqrt{C_{12}C_{21}}$$

Active coupling is characterized by complex values of β; furthermore, if consideration is given to coupling two waves with the same energy characteristics but opposite group velocities the power carried by the two lines is

$$P_1 = -|A_2(0)|^2 \frac{\sinh^2\beta_{12}(L-Z)}{\cosh^2\beta_{12}L} \tag{4}$$

$$P_2 = +|A^2(0)|^2 \frac{\cosh^2\beta_{12}(L-Z)}{\cosh^2\beta_{12}L} \tag{5}$$

Note that the power lost exponentially by line 2 causes the power in line 1 to increase exponentially in the minus Z direction. This condition defines active coupling. Conservation of total power is maintained and is independent of Z.

In the case of coupling two modes with differing phase constants, active coupling may be achieved by making the coupling coefficient in equations (1) and (2) periodic with the correct period. In general, solutions to problems of this type are quite difficult using the above techniques. A more practical approach is to consider the coupled lines as a periodic structure such as shown in Figure 2.

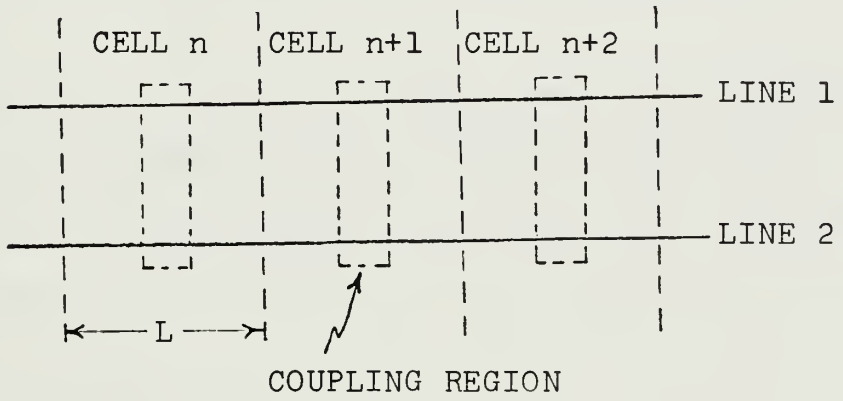

Figure 2. Periodically Coupled Lines.

In this case lines one and two are discretely coupled at points separated by distance L; thus over this coupling length, the number of cells times L, the lines may be considered as a series of coupled, unit cells. If conservation of energy and linearity are assumed, it may be shown, [3],

that for active coupling the coupled line equations may be written as

$$\begin{bmatrix} A_{n+1}^{(1)} \\ A_{n+1}^{(2)} \end{bmatrix} = \begin{bmatrix} \sqrt{1+k^2}\, e^{-j\theta_1} & +ke^{-j\theta_2} \\ +ke^{-j\theta_1} & \sqrt{1+k^2}\, e^{-j\theta_2} \end{bmatrix} \begin{bmatrix} A_n^{(1)} \\ A_n^{(2)} \end{bmatrix} \tag{6}$$

where

k = coupling coefficient

$\theta_{1,2}$ = phase shift across a unit cell on line 1,2

As shown in [4], solution of equation (6) results in

$$e^{-\gamma L} = \left[\sqrt{1+k^2}\,\cos\left(\frac{\theta_2-\theta_1}{2}\right) \pm \sqrt{(1+k^2)\cos^2\left(\frac{\theta_2-\theta_1}{2}\right)-1}\right] e^{-j\left(\frac{\theta_1-\theta_2}{2}\right)} \tag{7}$$

The propagation constant may take one of two forms depending on whether the term $(1+k^2)\cos^2\frac{\theta_2-\theta_1}{2}$ is less than or greater than unity. If this term is less than one, and assuming $k \ll 1$, then

$$\gamma_1 \doteq \frac{j\theta_2}{L} \tag{8}$$

$$\gamma_2 \doteq \frac{j\theta_1}{L} \tag{9}$$

In this case the waves are approximately those of the uncoupled lines. If, however, $(1+k^2)\cos^2\frac{\theta_2-\theta_1}{2} > 1$, the bracketed term in equation (7) is real and γ is complex. Letting $\frac{\theta_2-\theta_1}{2} = n\pi$ where $n = 1,2,\ldots$

$$e^{-\gamma L} = \left[\sqrt{1+k^2} \pm k\right] e^{-j\frac{(\theta_1+\theta_2)}{2}} \tag{10}$$

Again, if $k^2 \ll k$,

$$e^{-\gamma L} = e^{(\alpha+j\beta)L} \doteq [1 \pm k] e^{-j\left(\frac{\theta_1+\theta_2}{2}\right)} \tag{11}$$

The condition $\frac{\theta_2-\theta_1}{2} = n\pi$ adjusts the structure period such that active coupling will occur between waves having unequal phase constants and traveling in opposite directions. This condition is equivalent to

$$\beta_2 L - \beta_1 L = 2n\pi \tag{12}$$

If n = ±1 the required structure period for active coupling will be

$$L = \frac{2\pi}{|\beta_1-\beta_2|} = \frac{2\pi}{\Delta\beta} \tag{13}$$

2. Examination of Coupling Coefficient

The preceeding analysis required that the coupling coefficient be less than unity, i.e., $k^2 \ll k$. Physically this means that the coupling method used in the structure must not seriously perturb a traveling wave on a line from that which would exist were no coupling present. From equation (11)

$$\alpha L \doteq \pm k \tag{14}$$

Consequently at the interaction frequency

$$e^{-2\alpha(nL)} = P_d \tag{15}$$

where

n = the number of cells used for coupling

L = the structure period

P_d = the percent of total power remaining on the driven line

3. Examination of Exponential Power Transfer Between Coupled Lines

As previously mentioned, an exponential power transfer between two coupled lines defines active coupling. Refering again to equation (11), it is seen that $\alpha L = \pm k$ and

$$\beta L = \frac{\theta_1 + \theta_2}{2} \tag{16}$$

Again two waves propagate but, with active coupling, one wave decays exponentially while the other grows exponentially and the waves travel in opposite directions on the two lines.

The interaction between waves may be more clearly understood with the aid of an ω-β diagram discussed in the next section.

B. THE ω-β DIAGRAM

1. Determination of the ω-β Diagram

a. Theoretical Determination of the ω-β Diagram

Since experimental work dealt with coupling between a TEM wave on a coaxial line and a TE_{10} wave in a rectangular waveguide, the ω-β diagram for these structures will be considered. For a lossless, air filled rectangular waveguide, the expression relating ω and β is

$$\beta = \frac{\pm\omega\sqrt{1-\left(\frac{fc}{f}\right)^2}}{c} \qquad (17)$$

where

fc = the cutoff frequency

c = the velocity of light

The relationship for a lossless coaxial line is

$$\beta = \pm\omega\sqrt{LC} \qquad (18)$$

where

L = inductance per unit length

C = capacitance per unit length

The resultant ω-β diagrams from equations (16) and (17) are both plotted in Figure 3.

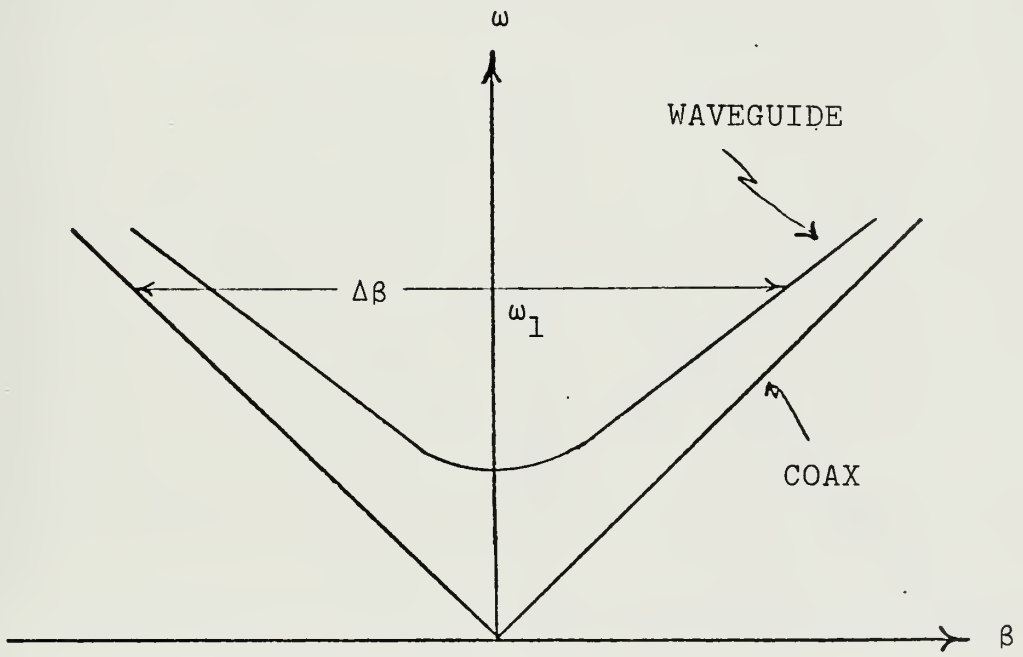

Figure 3. ω-β Diagram for Uncoupled Waveguide and Coaxial Lines.

Note that four linearly independent waves are represented in Figure 3: a forward and backward wave on both the waveguide and coaxial line. Refering to equation (13) active coupling at a given frequency may be achieved by adjusting the structure period, L, to $L = \frac{2\pi}{\Delta\beta}$ where $\Delta\beta$ at ω_1 is shown in Figure 3.

Coupling the two lines together periodically forms a structure which has an entirely different ω-β diagram from that directly obtainable from Figure 3. However, realizing that the coupled ω-β diagram has periodicity of $\frac{2\pi}{L}$ and that all information is contained in the Brilluoin zone, $-\frac{\Delta\beta}{2} \leq \beta < +\frac{\Delta\beta}{2}$, an approximate $\omega\beta$ diagram for the coupled strucutre may be obtained by translating the diagram of Figure 3 by $\Delta\beta$. This results in the diagram of Figure 4, which becomes more accurate as $k \to 0$.

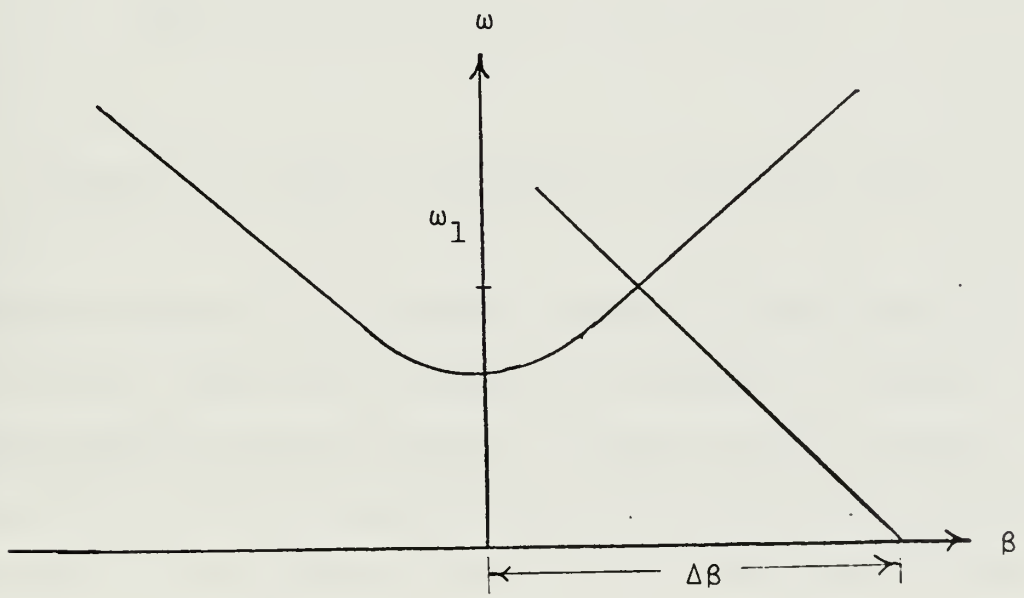

Figure 4. Approximate ω-β Diagram of Coupled Lines.

Figure 4 shows that for the $\Delta\beta$ shown, active coupling would be expected at ω_1, as described by the equations of the previous section.

A finite value of k results in the ω-β diagram of Figure 5.

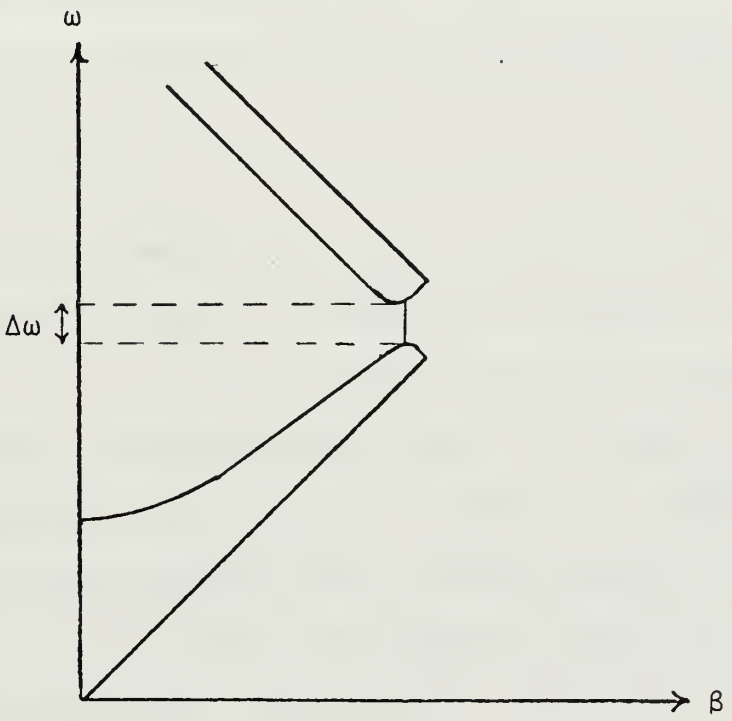

Figure 5. Exact ω-β Diagram of Coupled Lines.

The area of Figure 5 of primary interest is that shown by $\Delta\omega$. In this region the propagation constant is complex and active coupling can be expected. Away from this region, the real part of the propagation constant goes to zero and two waves will propagate as they would on uncoupled lines. A detailed analysis of degeneracies, stopbands, and symmetry arguments may be found in [4] and [5].

b. Experimental Determination of the ω-β Diagram

The most convenient and direct method of experimentally determining an ω-β diagram for a transmission line is to short one end of the line, drive the other end at a known frequency, and measure the resultant standing wave ratio. The distance between nulls (or peaks) is $\frac{\lambda}{2}$ and β at a given frequency may then be determined from

$$\beta = \frac{2\pi}{\lambda} \tag{19}$$

Plotting β for several different frequencies produces the ω-β diagram. It must be remembered, however, that if this is done for a coupling structure, then the structure must be intact for the measurement and that frequencies near the interaction frequency must be avoided. To avoid unwanted reflections and the resultant erroneous data, the coupled line which is not under investigation should be terminated in its characteristic impedance at both ends.

2. Application of the ω-β Diagram to Periodic Structures

The first step in applying the ω-β diagram to design of a periodic structure is judicious choice of Δβ. Referring to Figure 4, this is directly related to the desired frequency of interaction, which naturally must be considered. Of equal importance, however, is the fact that if Δβ is chosen too small an excessive number of crossings on the diagram may result making any meaningful analysis of the resultant interactions impossible.

Upon selection of a suitable Δβ the structure period may be determined from equation (13). Tolerances in the

physical structure itself become increasingly important as L decreases and consequently $\Delta\beta$ may be limited by available fabrication techniques.

II. EXPERIMENTAL INVESTIGATION

A. PERIODIC STRUCTURES INVESTIGATED

Two basic structure designs, each with two modifications, were investigated. These are shown in Figures 6-9.

1. Coupling Structures A and B

Coupling structures A and B were of the same basic design differing only in the geometry of the coupling method. The physical components of these structures were X-band waveguide with OD of 1.0 x 0.5 in. and a copper channel fabricated to fit over the large dimension of the waveguide. The approximate 1 x 1 in. dimensions of the channel dictated that a round center conductor with a diameter of 0.463 in. was necessary to form a coaxial transmission line with $Z_o = 50$. This rod was mounted in the center of the channel and both the rod and channel were tapered at one end to form a gradual transition region from RG-8A/U standard coaxial cable to the channel itself.

Holes were drilled in the waveguide in the patterns shown in Figures 6 and 7. For convenience the desired interaction frequency was chosen as 9 GHz which resulted in the following structure period:

$$\beta_{\substack{\text{BACK} \\ \text{COAX}}} = \omega\sqrt{\mu\varepsilon} = -188.7 \qquad (20)$$

$$\beta_{\substack{\text{FORWARD} \\ \text{WAVEGUIDE} \\ \text{TE}_{10}}} = \sqrt{\omega^2\mu\varepsilon - \left(\frac{\pi}{4}\right)^2} = 129.5 \qquad (21)$$

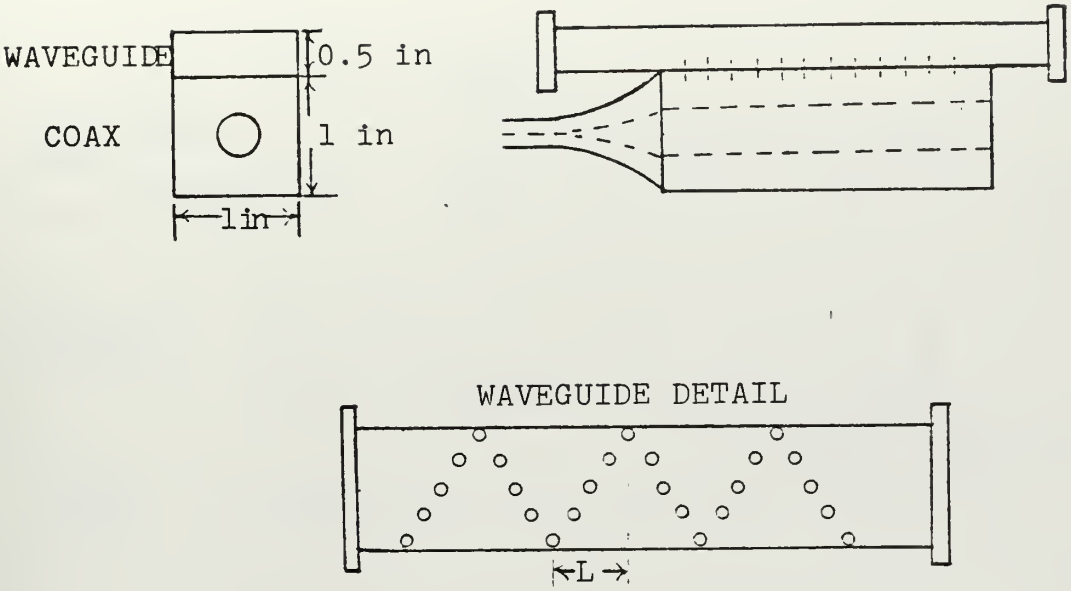

Figure 6. Coupling Structure A.

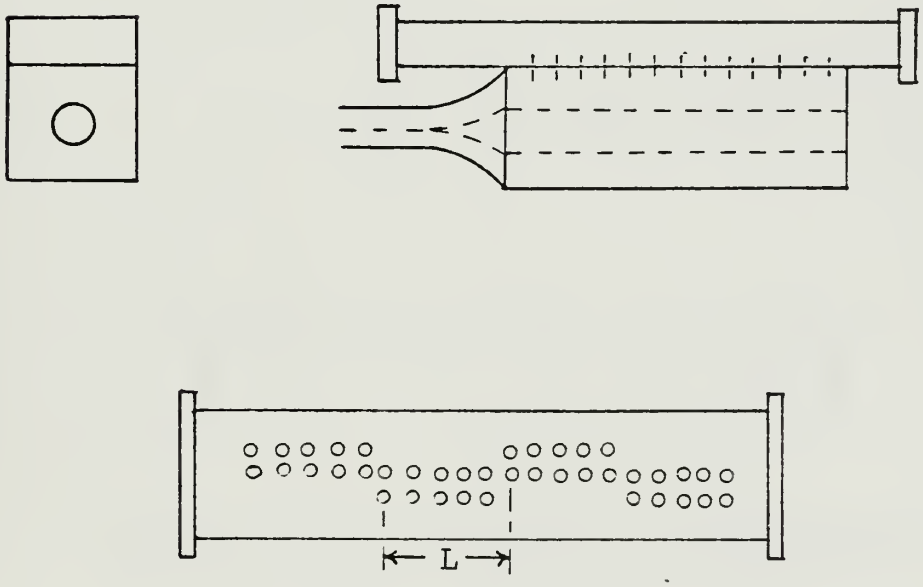

Figure 7. Coupling Structure B.

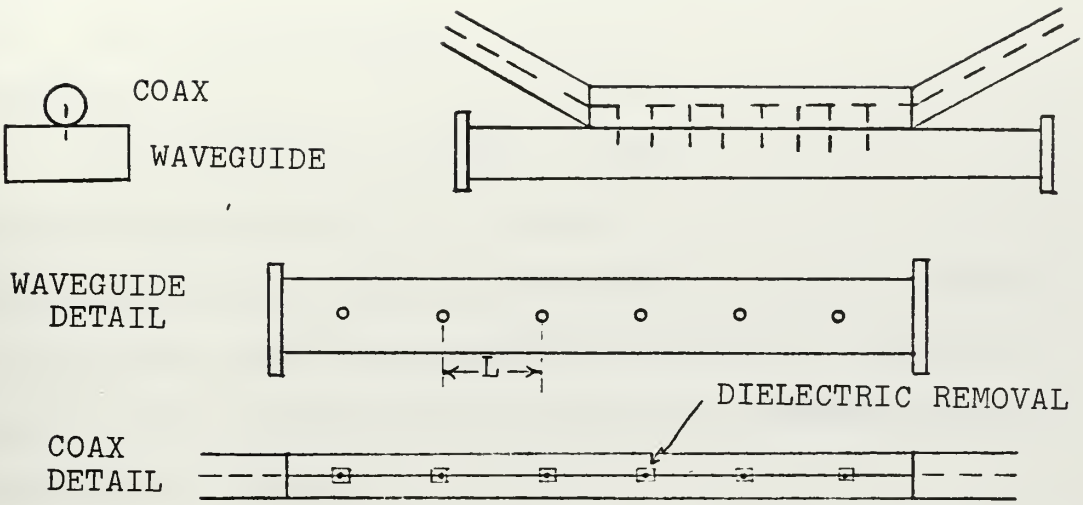

Figure 8. Coupling Structure C.

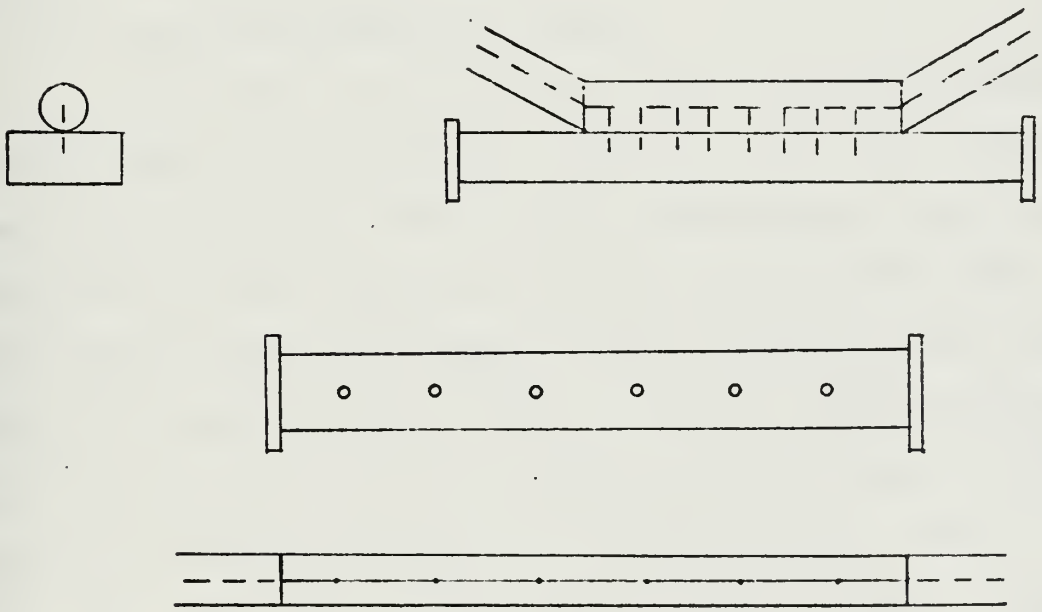

Figure 9. Coupling Structure D.

where

a = ID of waveguide = 0.9 in

Therefore

$\Delta\beta = (129.5) - (-188.7) = 318.2$

and from Equation (13), $L = 2.9$ cm.

This period was the same in structures A and B. However, in structure B the hole pattern was altered as shown in Figure 7; the parallel rows of holes were spaced 0.25 in. from center to center.

Slots were machined in the center of both the waveguide and channel to allow slotted line measurements. Both ends of the waveguide were fitted with waveguide flanges and the tapered end of the channel was terminated in a standard type N coaxial connector.

2. Coupling Structures C and D

The design of structures C and D is quite similar to each other but considerably different from the structures previously discussed. The coaxial transmission line used in structures C and D was made directly from RG-8A/U cable. The braided shield was removed from a section of the standard cable and replaced by a section of 3/8 in. copper tubing which had a 1/16 in slot cut along its full length. This produced a section of continuous RG-8A/U cable, part of which was rigid. The slot in the tubing allowed probes to pass from the inner conductor of the cable through the outer conductor and into the waveguide through appropriately spaced holes drilled in the waveguide. The waveguide therefore

required only a series of centerline holes spaced at the proper period.

The period for structure C was chosen as L = 7.24cm simply because existing waveguide with centerline holes at this spacing was available. Probe attachment to the coaxial cable was made by cutting away enough of the RG-8A/U polyethelene dielectric to allow the soldering of a wire probe to the center conductor which extended 15/64 in. into the waveguide.

Structure D differed from structure C in that the designed period of the structure was L = 1.5707 cm. The probe attachment was made by driving a probe through the dielectric to the center conductor and thus required no dielectric removal. Varying probe lengths were investigated with structure D.

B. MEASUREMENT TECHNIQUES

1. The Standing Wave Ratio Measurement

All SWR measurements were made using a Hewlett-Packard 415-A square law detector with crystal detector. To facilitate this measurement, 1/8 in. slots were machined in the copper channel and waveguides of structures A and B and a 1/16 in. slot was machined in the copper tubing and waveguide of structures C and D.

2. The Power Measurement

By far the most important measurement in connection with this investigation was that of the power from each of

the four ports of coupling structures C and D. The technique is shown in Figure 10.

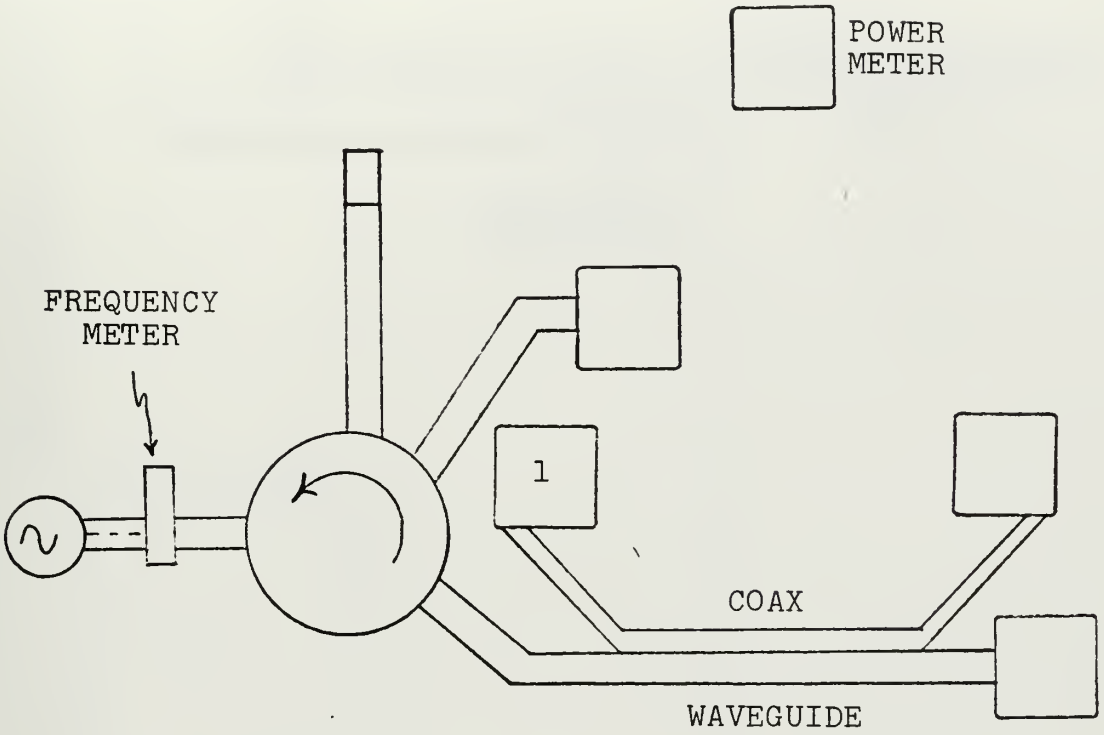

Figure 10. Power Measurement Method.

This measurement technique terminated the four ports in their characteristic impedance with the resultant reduction in reflections and furthermore provided complete information about power distribution at any given frequency. It may be seen from Figure 10 that these measurements were taken by driving the waveguide and coupling the power to the coaxial line, measured by power meter 1.

3. The Swept Frequency Measurement

An overall view of coupled power was obtained using swept frequency techniques covering the frequency range from 8 GHz to 11.7 GHz. Figure 11 shows the swept frequency measurement technique.

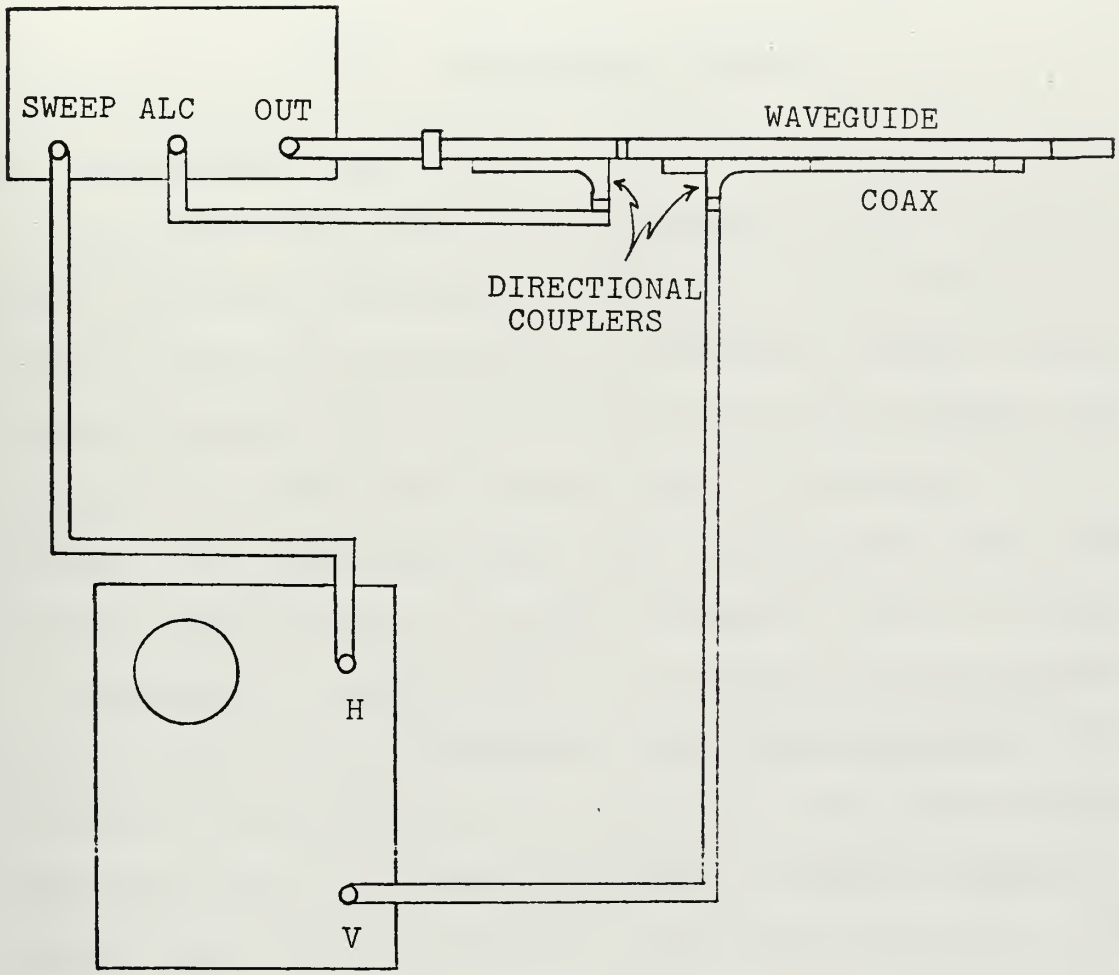

Figure 11. Swept Frequency Measurement Method.

The results of this measurement show the relative power distribution over the swept frequency range. Although not as accurate or detailed as the point by point power measurements taken, they are an excellent indicator of overall coupling action.

III. EXPERIMENTAL RESULTS

A. UNSUCCESSFUL STRUCTURES

The measurements made with structures A and B did not verify the theory discussed in Section I. The intent was to drive either the waveguide or the copper channel coaxial line and measure the coupled power out of the undriven line as well as its SWR. The coupled power on structure A was extremely low which indicated that the waveguide hole pattern required modification to provide stronger H field coupling.

Although the coupled power of structure B was somewhat greater than that of structure A, the SWR measurements fell far short of approaching the exponential power curve expected along the line. It is believed that the copper channel coaxial line used in structures A and B was not built to the tolerances required. Furthermore it was determined that the cost of fabricating such a precision device was not warranted which led to consideration of an entirely different coupling method.

This led to the construction of structure C previously described. Approximately 1/4 in. of insulation was removed for each of the five probes used. Power measurements were then taken using the method shown in Figure 10. The normalized power measurements are shown in Figure 12.

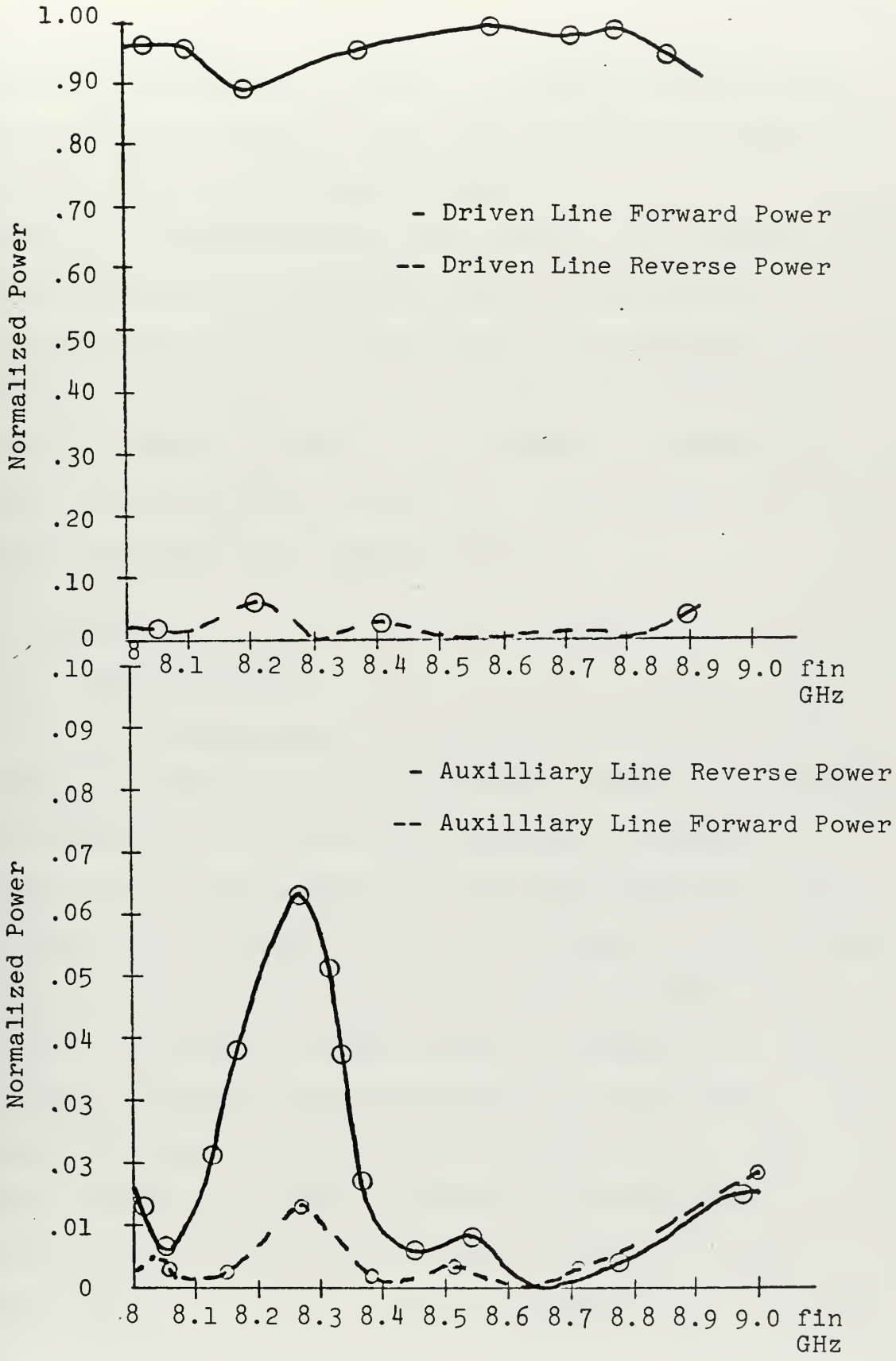

Figure 12. Normalized Power for Coupling Structure C
Probe Length = 0.125 in.

Referring to Figure 12 it may be seen that the greatest interaction occurs at 8.25 GHz. It will be recalled that the period of structure C was 7.24 cm and from equation (13) $\Delta\beta = 87$. From an ω-β diagram analysis an interaction at 8.2 GHz was expected which corresponded to the fourth crossing of coaxial ω-β curve with that of the waveguide.

The relatively low coupled power was attributed primarily to two causes. First, the dielectric removal for probe attachment introduced a considerable discontinuity in the coaxial line and second the structure had only five probes throughout the coupling region.

B. STRUCTURE D

1. Coupled Power

The shortcomings of structure C were overcome by changing the method of probe attachment previously described and increasing $\Delta\beta$ to 400 which increased the number of probes to 21. The resultant power measurements for three different probe lengths are shown in Figures 13-15. It may be seen that structure D coupled from 82% to 99% of the power as a function of probe length. Figures 16-18 show the swept frequency power measurement for structure D. The frequency range is from 8 GHz to 11.7 GHz in each case. The first marker is at 8 GHz; in Figure 16, probe length = 0.062 in., the second marker is at 9.50 GHz, in Figure 17, probe length = 0.125 in., the second marker is at 9.45 GHz, and in Figure 18, probe length = 0.187 in., the second marker

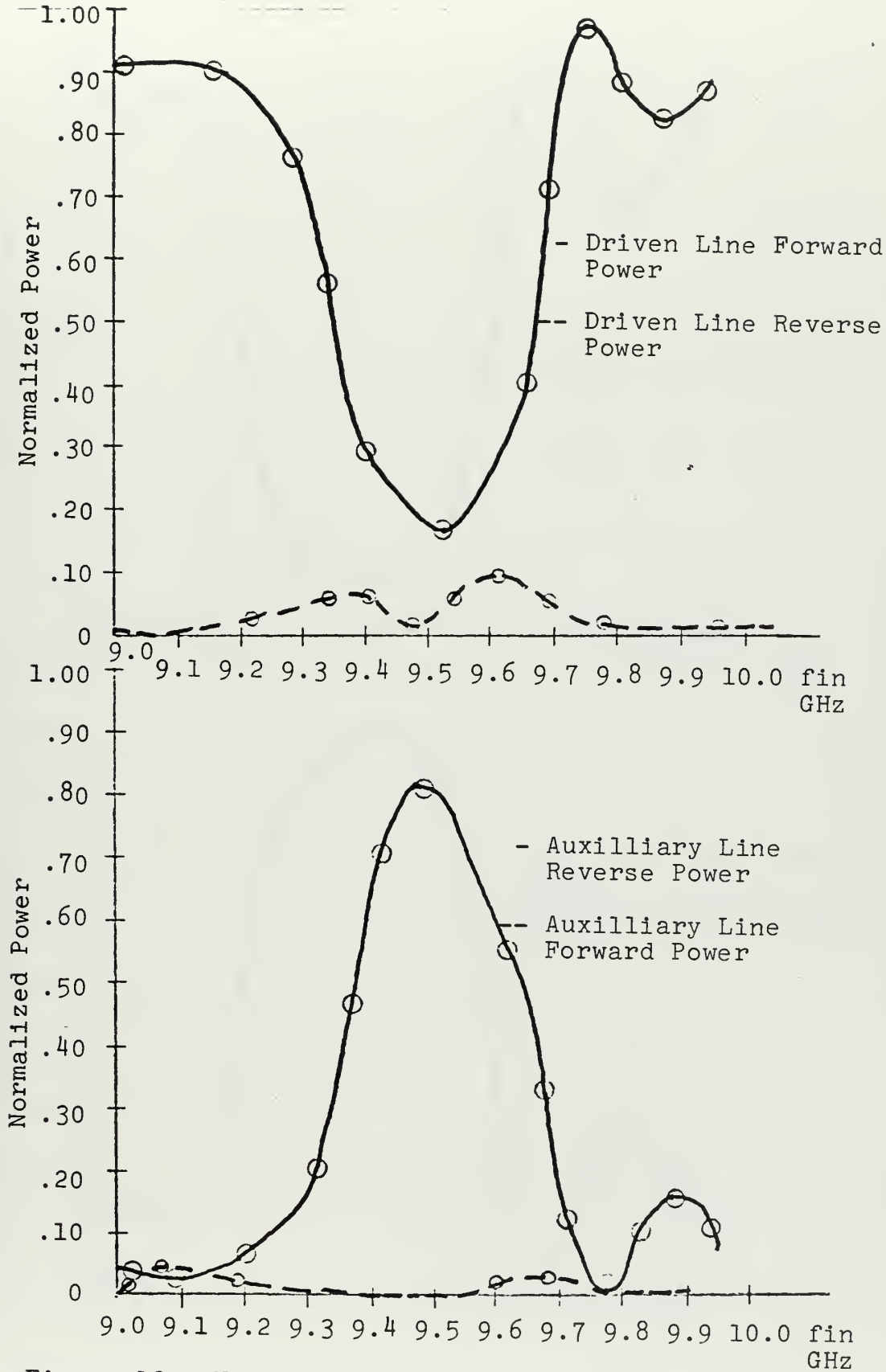

Figure 13. Normalized Power for Coupling Structure D Probe Length = 0.062 in.

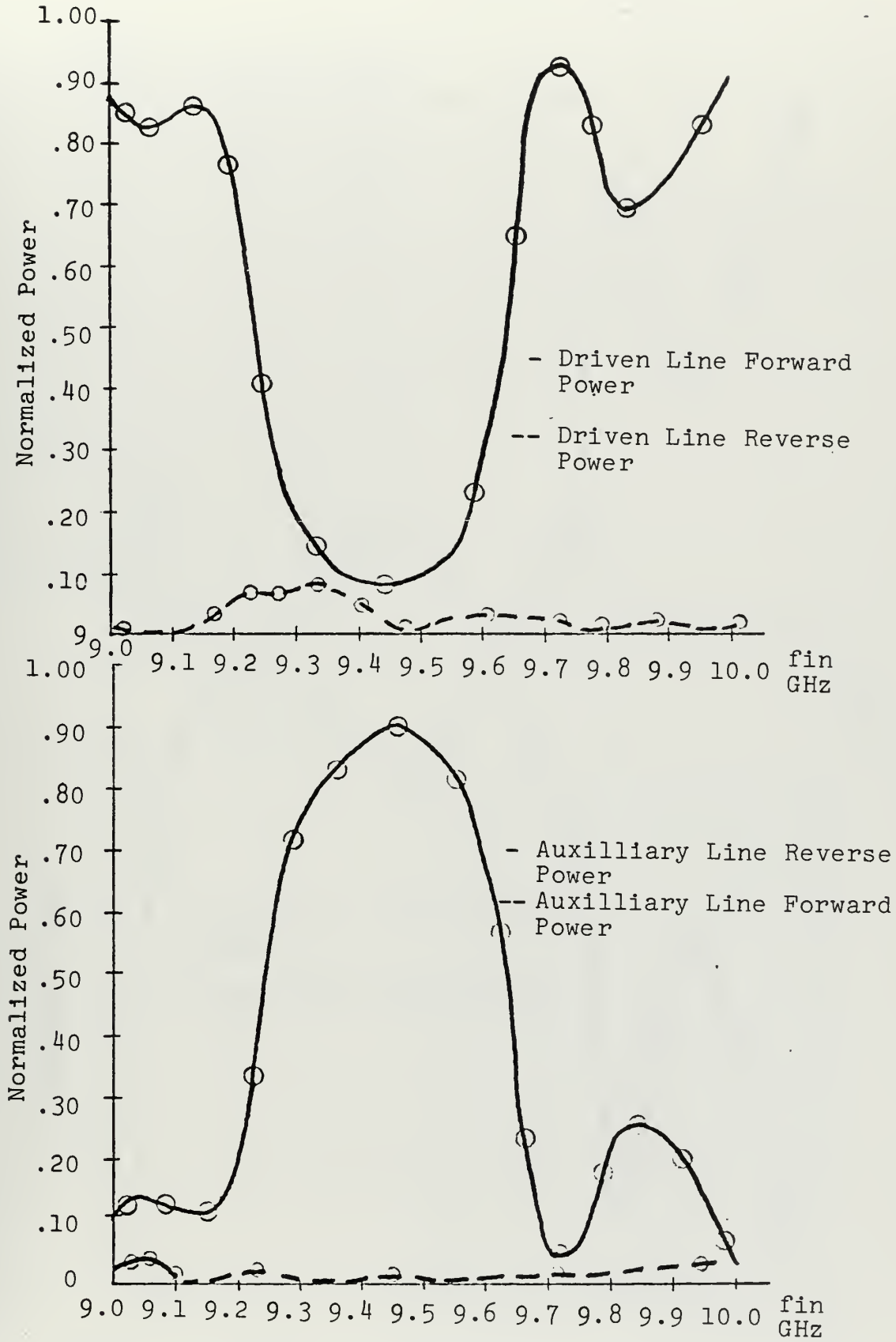

Figure 14. Normalized Power for Coupling Structure D Probe Length = 0.125 in.

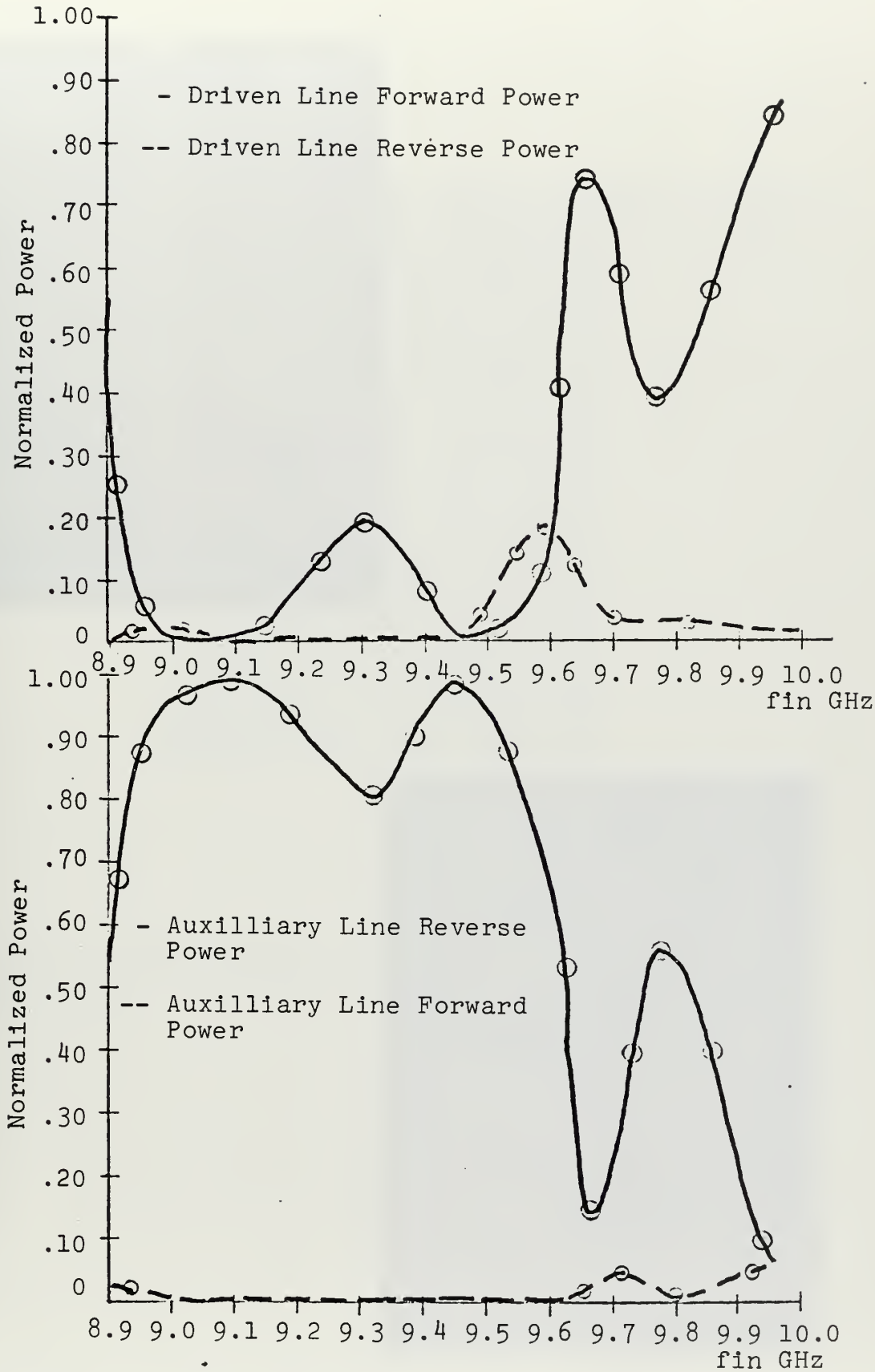

Figure 15. Normalized Power for Coupling Structure D
Probe Length = 0.187 in.

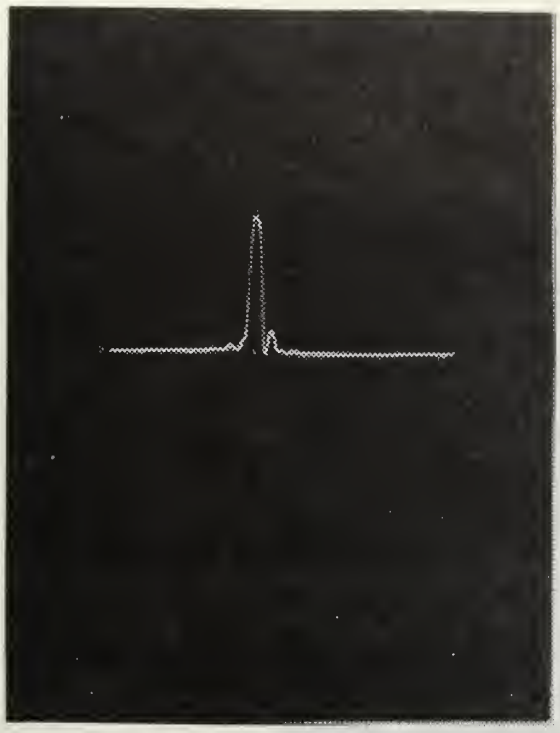

Figure 16. Swept Frequency for Coupling Structure D
Probe Length = 0.062 in.

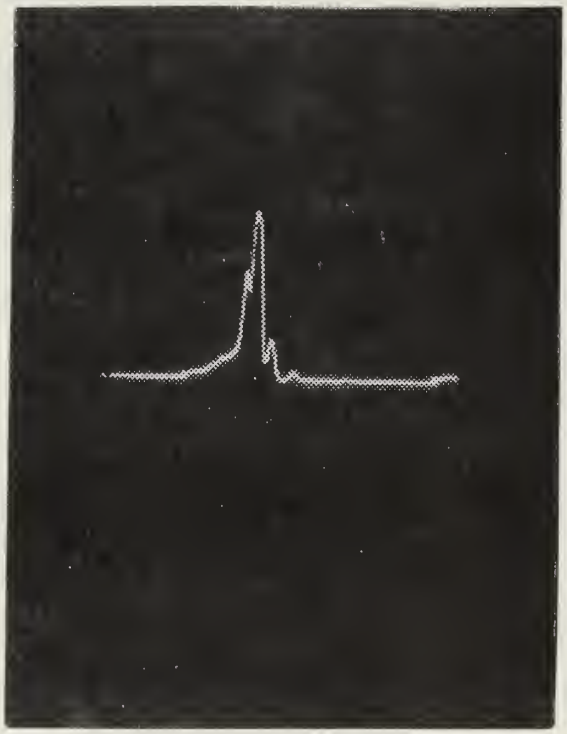

Figure 17. Swept Frequency for Coupling Structure D
Probe Length = 0.125 in.

is at 9.275 GHz. To facilitate further investigation, complete data for Figures 13-15 has been included in Appendix A.

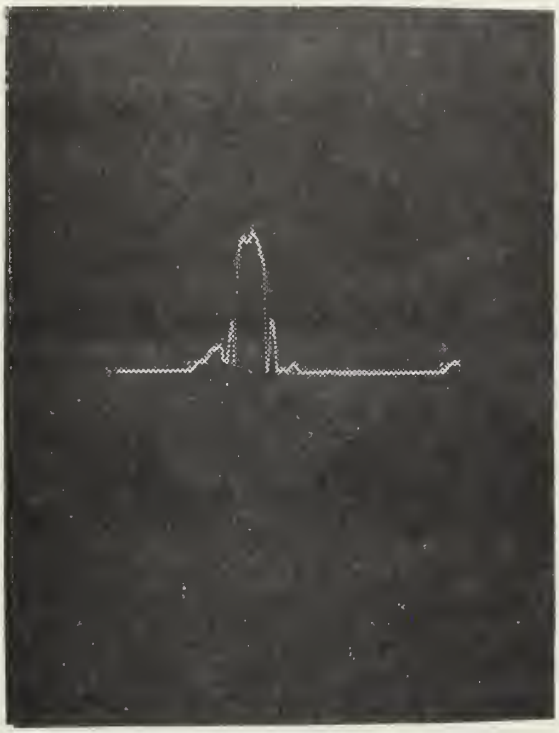

Figure 18. Swept Frequency for Coupling Structure D
Probe Length = 0.187 in.

To obtain a more meaningful representation of the coupled power ratio to incident driven port power, rather than total power, Figures 19-21 have been included for the three probe lengths investigated.

2. Coupling Coefficient

The coupling coefficient for the varying probe lengths of structure D may be calculated from equations 14 and 15. If this is done for the three probe lengths investigated it is found that for

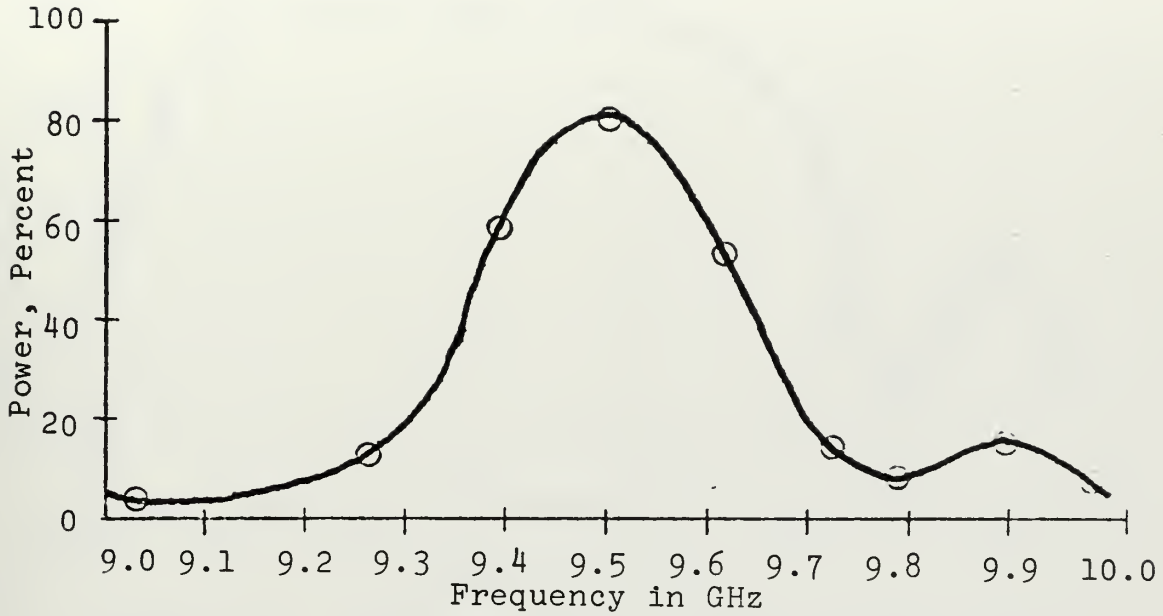

Figure 19. Ratio of Coupled Power to Input Power
Probe Length = 0.062 in.

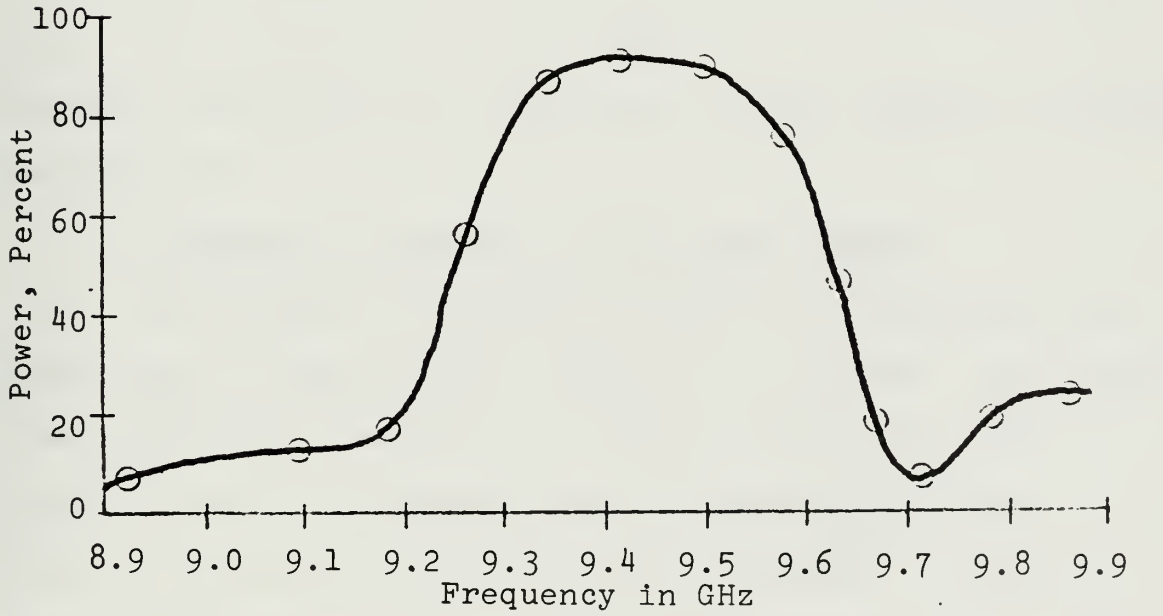

Figure 20. Ratio of Coupled Power to Input Power
Probe Length = 0.125 in.

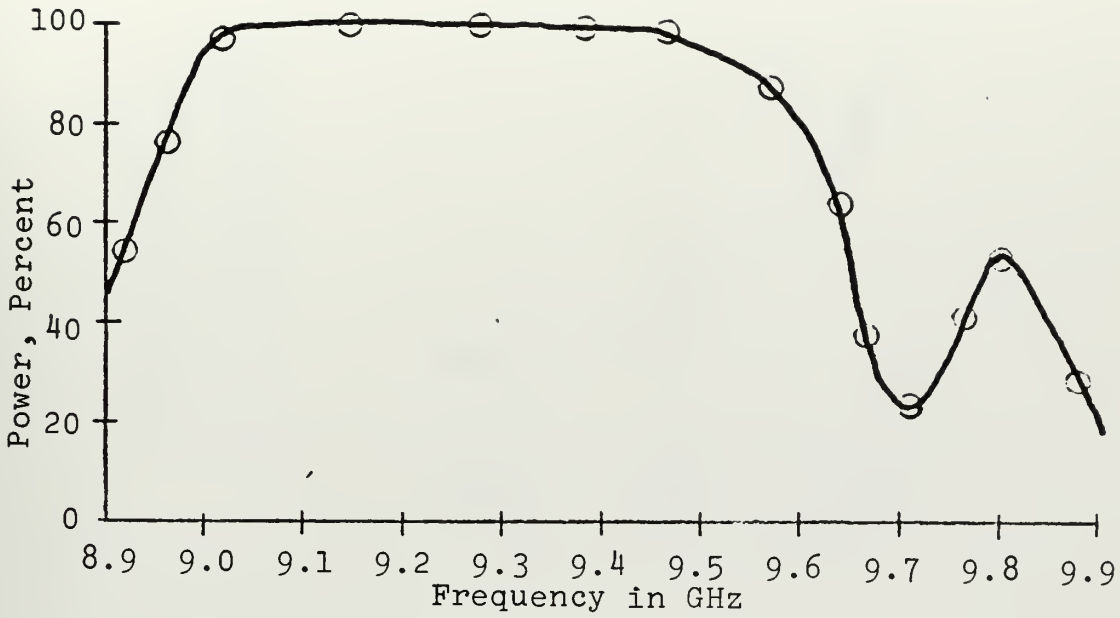

Figure 21. Ratio of Coupled Power to Input Power
Probe Length = 0.187 in.

L = 0.062 in., K = 0.0431

L = 0.125 in., K = 0.0573

and L = 0.187 in., K = 0.141

Coupling coefficient as a function of probe length is plotted in Figure 22.

3. Summary of Variations with Probe Length

In addition to coupling coefficient variation with probe length several other affects may be noted. The coupled power bandwidth increases with increasing probe length as does the amount of coupled power. Longer probes also increase the reflected power in the waveguide. Figure 23 shows the change in 3 db coupled power bandwidth as a function of probe length. Figure 24 shows change in peak coupled power as a function of probe length.

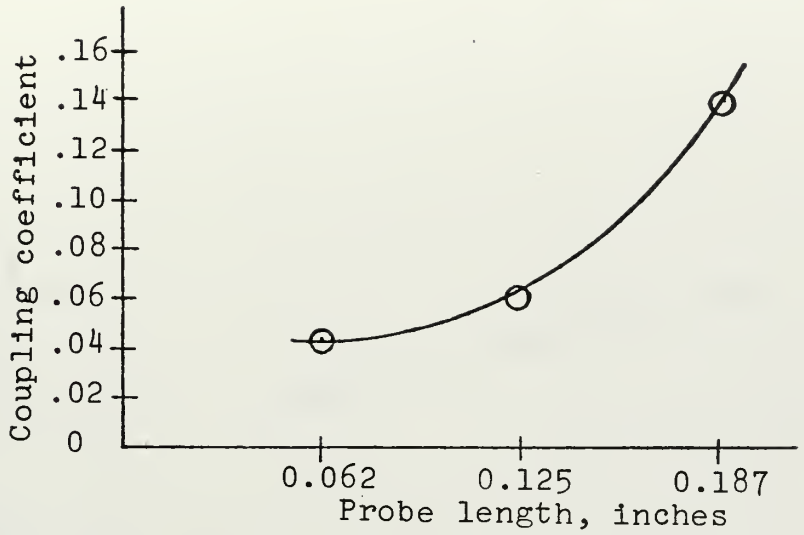

Figure 22. Coupling Coefficient as a Function of Probe Length.

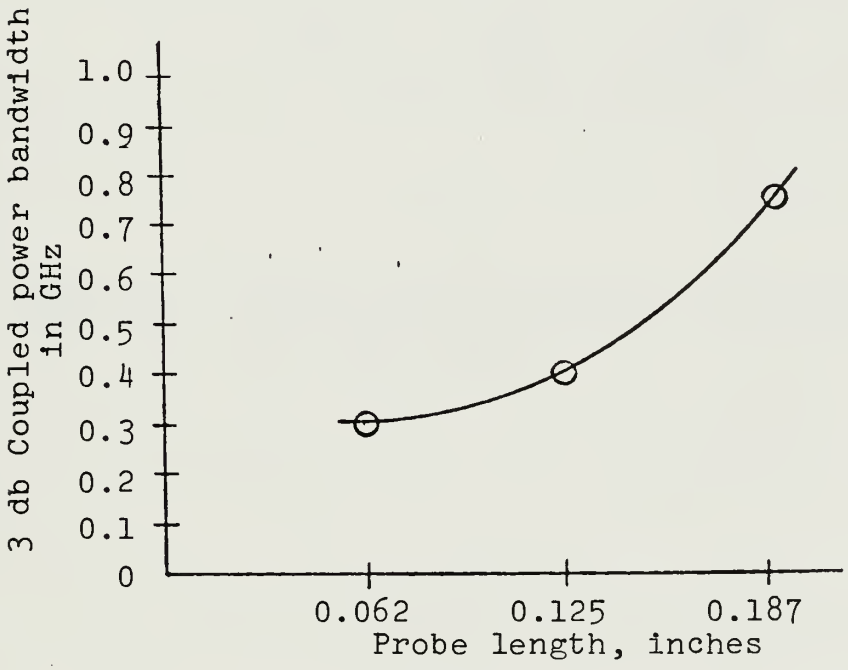

Figure 23. Coupled Power Bandwidth as a Function of Probe Length.

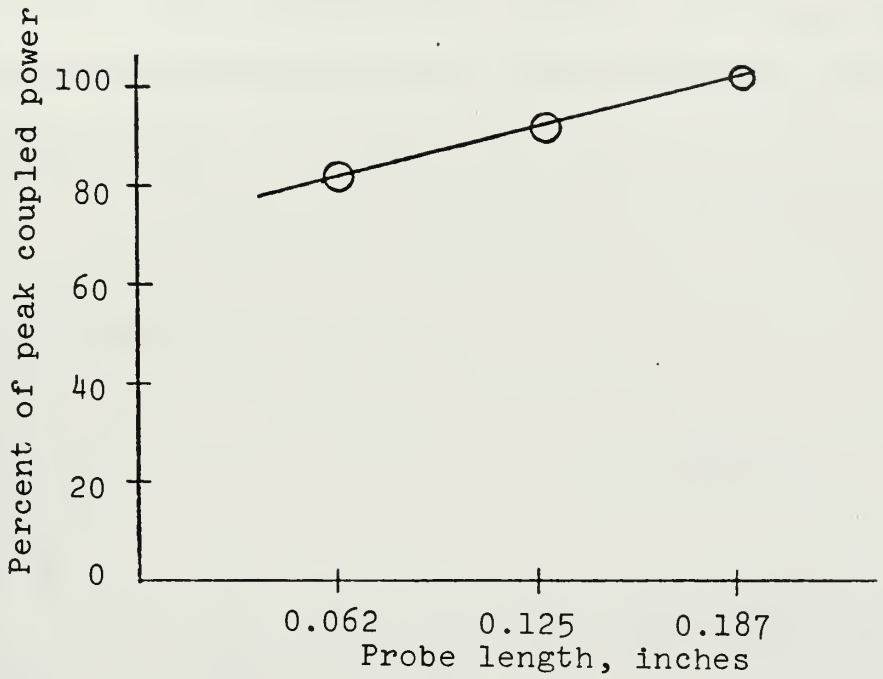

Figure 24. Peak Coupled Power as a Function of Probe Length.

4. Decay and Growth of Coupled Waves

The standing wave ratio along the lengths of both the waveguide and coaxial line were measured to verify the exponential decay and growth of the coupled waves. The results are shown in Figure 25 where P_1 represents the power on the driven line and P_2 represents the power on the coupled line.

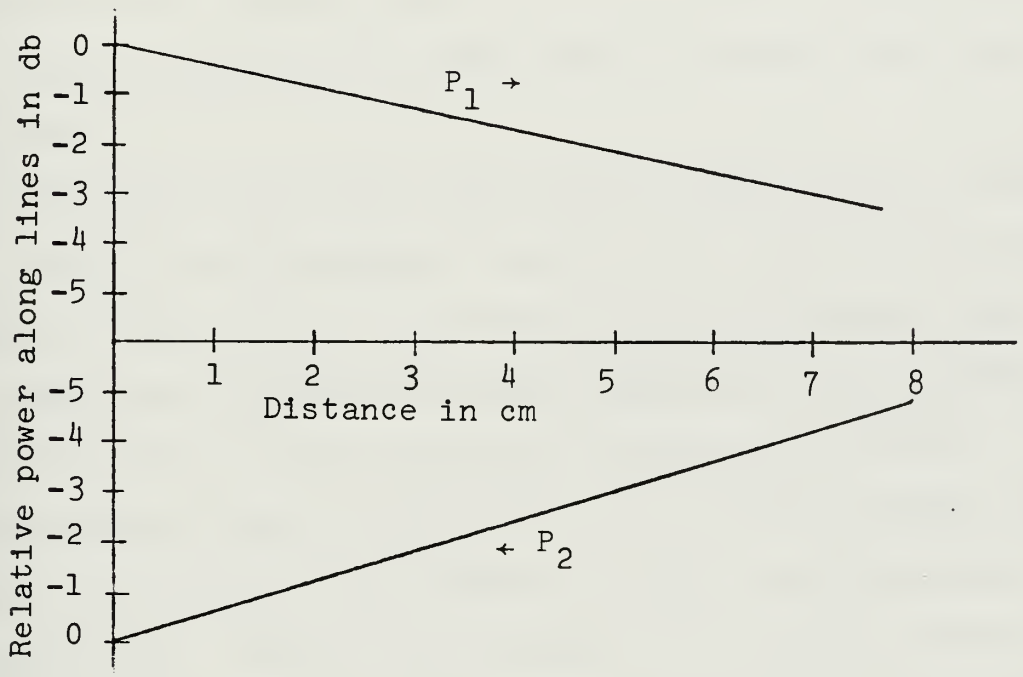

Figure 25. Exponential Power Change Between Coupled Lines.

It may be seen that over the short section of the structure measured, the wave amplitudes on the driven and coupled lines do exhibit the necessary exponential decay and growth.

5. Interaction Frequency

The interaction frequency of 9.45 GHz was considerably higher than the 8.75 GHz crossover point for the ω-β branches of the uncoupled lines. ω-β measurements of the waveguide for structure D indicated that it had not been perturbed. The structure $\Delta\beta$ was measured as 402, very close to the design of 400. It was apparent that the coaxial structural modifications had changed the nominal RG-8A/U phase velocity from 0.66 c to 0.76 c. Repeated experimental measurements were taken to verify this phase velocity.

The method previously described to obtain an ω-β diagram for a device was attempted. However, the slot in the copper tubing of the coaxial line behaved as a slot antenna and the resultant radiation obscured meaningful measurements. A modification of this method was attempted by using a small hole in place of the slot in the coaxial tubing. The intent was to adjust the frequency until a null appeared at this hole. However, the tuning of the crystal detector varied too broadly over the frequency band and an accurate null could not be obtained. Finally, a cavity was constructed from copper tubing and RG-8A/U cable and an attempt was made to measure the resonant points of the cavity. A suitable method of driving the cavity could not be fabricated and the resultant reflections nullified any resonance measurements.

The resultant shift in interaction frequency was attributed to inductive loading of the coaxial line caused by the insertion of probes. An impedance measurement was made with a length of standard RG-8A/U cable loaded with a single probe.

The results of this measurement produced a probe admittance of $y = 0.1 - j0.4$. The real part of this admittance is that due to probe radiation into the waveguide. The inductive susceptance measured raises the phase velocity of the coaxial cable from 0.66 c to 0.76 c which results in the interaction frequency of 9.45 GHz. Figure 26 shows the theoretical ω-β diagram of coupling structure D together with experimentally measured points. Also included is the measured attenuation constant.

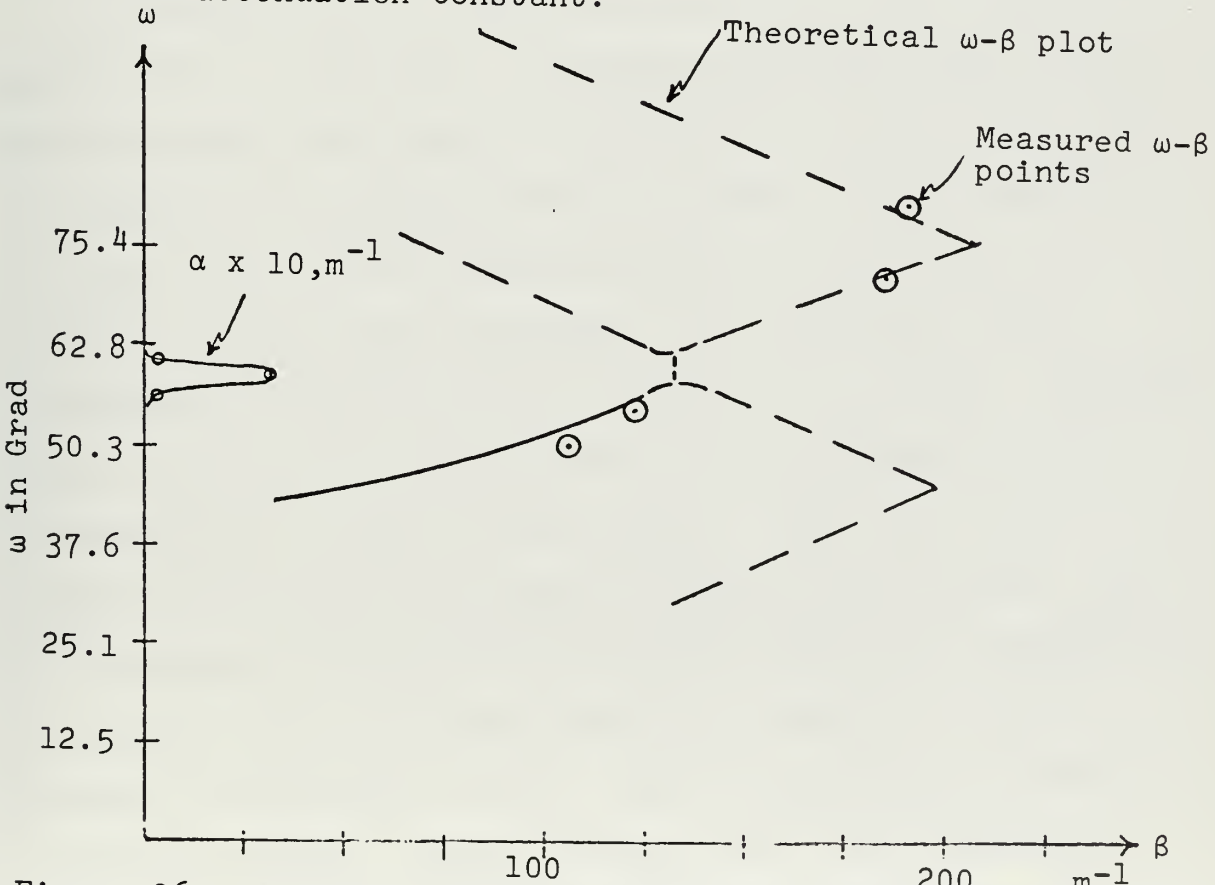

Figure 26. Measured α and ω-β Points for Coupling Structure D.

IV. CONCLUSIONS AND RECOMMENDATIONS

This thesis has experimentally verified several aspects of the theory of periodic coupling of modes of propagation. Specifically, it has shown that energy may be transferred between two coupled lines carrying waves with differing phase constants. The defining criteria of active coupling characterized by an exponential decay of the wave amplitude on the driven line and the corresponding growth of wave amplitude on the coupled line were observed. Coupling coefficient, power transfer, and bandwidth as a function of probe length were investigated.

A structure of the type described could have immediate application as a filter. By making the probe length small and increasing the number of periods to a point sufficient to transfer the required amount of power, it is reasonable to expect that a very narrow bandwidth filter could be designed for any given frequency. The bandwidth would ultimately be limited only by losses in the system. Furthermore, new insight to this problem could perhaps be gained by analyzing it from a filter aspect. Much work has, of course, been done in the area of directional filters, that is frequency selective devices which combine the properties of filters and directional couplers. Several of these devices are discussed in [6] - [8]. None employ periodic coupling, however, and the general strip line techniques used offer no possibility of broad band capabilities.

The ultimate goal of any future investigation should be to construct a broadband coupler using log periodic coupling. This is further described in [4], but the general concept is that which has been successfully applied to antennas. By scaling the period of the coupling throughout the coupling region, it is expected that active coupling could be achieved over a broad frequency range.

APPENDIX A

POWER MEASUREMENT DATA FOR COUPLING STRUCTURE D

The data taken for plotting the normalized power of coupling structure D, Figures 13-15, is presented below to aid in further investigations.

Probe Length = 0.062 in.

f GHz	Driven Line Backward Power		Driven Line Forward Power		Coupled Line Backward Power		Coupled Line Forward Power	
	mw	%	mw	%	mw	%	mw	%
9.002	0.039	0.48	7.30	91.26	0.340	4.25	0.320	1.28
9.055	0.026	0.35	6.80	91.87	0.255	3.44	0.320	4.32
9.117	0.018	0.42	3.80	91.88	0.150	3.62	0.168	4.06
9.17	0.034	0.68	4.50	91.20	0.236	4.78	0.164	3.32
9.19	0.086	1.39	5.50	89.41	0.380	6.17	0.185	3.00
9.234	0.230	3.07	6.40	85.44	0.680	9.07	0.180	2.4
9.298	0.225	3.86	4.50	77.38	0.98	16.85	0.110	1.89
9.348	0.310	5.75	3.10	57.56	1.92	35.65	0.55	1.02
9.388	0.380	7.00	1.90	35.39	3.10	57.14	0.025	0.46
9.451	0.080	2.91	1.10	20.03	4.30	78.30	0.012	0.20
9.480	0.018	0.40	0.78	16.95	3.80	82.59	0.002	0.05
9.515	0.110	3.20	0.52	15.12	2.80	81.46	0.007	0.20
9.556	0.233	7.91	0.58	19.69	2.10	71.31	0.032	1.06
9.598	0.400	10.76	0.98	26.37	2.25	60.54	0.86	2.31
9.645	0.410	9.07	1.61	35.63	2.34	51.79	0.158	3.49
9.718	0.019	0.56	2.91	83.46	0.49	14.05	0.067	1.92
9.755	0.017	0.39	4.20	98.47	0.06	0.14	0.042	0.98
9.770	0.022	0.47	4.60	97.89	0.28	0.60	0.048	1.02
9.780	0.026	0.53	4.80	96.37	0.10	2.00	0.054	1.08
9.797	0.036	0.69	4.80	92.28	0.30	5.86	0.060	1.15
9.840	0.050	0.79	5.20	83.01	0.95	15.16	0.064	1.02
9.917	0.009	0.17	4.00	81.53	0.84	17.12	0.057	1.16
9.949	0.064	1.11	5.10	89.14	0.48	8.39	0.077	1.34

Probe Length = 0.125 in.

f GHz	Driven Line Backward Power		Driven Line Forward Power		Coupled Line Backward Power		Coupled Line Forward Power	
	mw	%	mw	%	mw	%	mw	%
9.021	0.007	0.08	6.70	83.62	0.99	12.29	0.32	3.99
9.055	0.015	0.21	5.60	81.57	0.95	13.83	0.30	4.37
9.086	0.025	0.53	3.40	83.42	0.61	13.04	0.14	2.99
9.126	0.021	0.58	3.10	86.51	0.44	12.37	0.02	0.61
9.151	0.055	1.54	3.05	86.50	0.42	11.91	0.00	0.04
9.164	0.105	2.80	3.20	85.53	0.42	11.22	0.02	0.43
9.184	0.240	5.39	3.55	79.80	0.58	13.03	0.08	1.76
9.200	0.345	6.64	3.80	73.17	0.92	17.71	0.13	2.46
9.214	0.390	6.98	3.65	65.40	1.40	25.08	0.14	2.52
9.236	0.355	6.67	2.71	50.93	2.15	40.04	0.11	1.94
9.264	0.300	6.30	1.56	32.77	2.85	59.88	0.05	1.04
9.287	0.300	6.70	1.00	22.35	3.15	70.40	0.02	0.53
9.324	0.365	8.29	0.58	13.06	3.45	78.39	0.01	0.24
9.365	0.375	8.03	0.44	9.32	3.85	82.52	0.00	0.11
9.401	0.240	4.71	0.43	8.35	4.42	86.87	0.00	0.05
9.43	0.088	1.65	0.42	7.91	4.80	90.40	0.00	0.02
9.462	0.021	0.43	0.39	7.95	4.43	91.56	0.00	0.04
9.441	0.049	1.24	0.35	8.96	3.50	89.68	0.00	0.10
9.525	0.076	2.53	0.33	10.84	2.59	86.40	0.00	0.21
9.559	0.082	2.97	0.38	13.80	2.28	82.83	0.01	0.37
9.596	0.080	2.33	0.82	23.96	2.50	73.06	0.02	0.62
9.630	0.091	1.98	2.14	46.72	2.30	50.21	0.05	1.06
9.655	0.120	2.49	3.12	64.91	1.50	31.21	0.07	1.37
9.71	0.116	2.77	3.90	93.36	0.12	2.82	0.04	1.02
9.737	0.051	1.09	4.40	94.07	0.19	3.99	0.04	0.83
9.761	0.018	0.33	4.60	86.95	0.61	11.53	0.06	1.18
9.780	0.016	0.28	4.60	80.64	1.00	17.53	0.09	1.53
9.805	0.048	0.76	4.60	73.98	1.46	23.48	0.11	1.76
9.830	0.100	1.49	4.65	69.40	1.82	27.16	0.13	1.94
9.880	0.100	1.56	4.55	71.13	1.60	25.01	0.15	2.28
9.925	0.032	0.62	4.00	77.94	0.96	18.70	0.14	2.72
9.996	0.017	0.33	4.20	84.56	0.60	12.08	0.15	3.02
10.004	0.009	0.15	5.40	92.41	0.25	4.19	0.19	3.23

Probe Length = 0.187 in.

f GHz	Driven Line Backward Power		Driven Line Forward Power		Coupled Line Backward Power		Coupled Line Forward Power	
	mw	%	mw	%	mw	%	mw	%
8.636	0.01	0.13	8.60	84.52	0.86	8.45	0.70	6.88
8.678	0.10	1.36	6.20	87.23	0.60	8.44	0.21	2.95
8.704	0.29	4.71	4.90	78.07	1.05	16.73	0.03	0.47
8.743	0.29	3.94	3.80	52.47	3.10	42.81	0.06	0.75
8.780	0.02	0.17	4.40	49.63	4.30	48.50	0.15	1.69
8.816	0.27	2.68	5.00	49.37	4.80	47.40	0.05	0.53
8.871	0.39	5.40	5.30	73.40	1.14	15.78	0.39	5.40
8.900	0.34	0.47	2.75	38.40	4.20	58.65	0.18	2.45
8.950	0.16	1.72	0.40	4.46	8.40	93.66	0.01	0.14
9.025	0.17	1.68	0.06	0.64	9.62	97.66	0.00	0.00
9.111	0.01	0.19	0.02	0.29	5.10	99.51	0.00	0.00
9.177	0.27	4.06	0.01	0.19	6.40	95.73	0.00	0.00
9.220	1.10	11.32	0.01	0.14	8.60	88.52	0.00	0.00
9.326	1.50	19.95	0.01	0.19	6.00	79.83	0.00	0.01
9.404	0.49	5.89	0.02	0.27	7.80	93.80	0.00	0.02
9.452	0.01	0.13	0.04	0.50	8.20	99.34	0.00	0.01
9.496	0.29	4.79	0.06	0.99	5.70	94.21	0.00	0.00
9.552	0.65	15.15	0.14	3.14	3.50	81.58	0.00	0.11
9.605	0.96	19.35	0.66	13.30	3.30	66.54	0.04	0.78
9.657	0.37	9.00	3.10	75.42	0.54	13.13	0.10	2.43
9.702	0.15	3.37	3.00	69.42	0.97	2.44	0.21	4.74
9.750	0.22	3.87	2.24	39.47	3.10	54.62	0.12	2.02
9.794	0.21	3.15	2.60	39.10	3.80	57.16	0.04	0.57
9.860	0.27	3.63	4.20	57.65	2.50	34.31	0.32	4.39
9.960	0.16	2.77	4.80	85.94	0.25	4.47	0.28	6.80

BIBLIOGRAPHY

1. Pierce, J. R., "Coupling of Modes of Propagation," Journal of Applied Physics, v. 25, p. 179-183, February, 1954.

2. Johnson, C. C., Field and Wave Electrodynamics, p. 296-306, McGraw-Hill, 1965.

3. Watkins, D. A., Topics in Electromagnetic Theory, p. 66-77, Wiley, 1958.

4. United States Naval Postgraduate School Report NPS-52K071081A, Periodic and Log Periodic Coupling of Modes of Propagation, by J. B. Knorr, p. 4, August 1971.

5. Knorr, J. B., Electromagnetic Applications of Group Theory, Ph.D. Thesis, Cornel University, 1970.

6. Coale, F. S., "A Traveling-wave Directional Filter," IRE Transactions on Microwave Theory and Techniques, p. 256-260, October 1956.

7. Wanselow, R. D. and Tuttle, L. P., Jr., "Practical Design of Strip-Transmission-Line Half-Wavelength Resonator Directional Filters," IRE Transactions on Microwave Theory and Techniques, p. 168-173, January 1959.

8. Cohn, S. B. and Coale, F. S., "Directional Channel-Separation Filters," Proceedings of the IRE, p. 1018-1024, August 1956.

INITIAL DISTRIBUTION LIST

		No. Copies
1.	Defense Documentation Center Cameron Station Alexandria, Virginia 22314	2
2.	Library, Code 0212 Naval Postgraduate School Monterey, California 93940	2
3.	Asst. Professor J. B. Knorr, Code 52ko Department of Electrical Engineering Naval Postgraduate School Monterey, California 93940	1
4.	Asst. Professor R. W. Adler, Code 52 Ab Department of Electrical Engineering Naval Postgraduate School Monterey, California 93940	1
5.	LT Albert E. Whitehead, USN 3166 Crescent Ave. Marina, California 93933	1

UNCLASSIFIED

Security Classification

DOCUMENT CONTROL DATA - R & D

(Security classification of title, body of abstract and indexing annotation must be entered when the overall report is classified)

1. ORIGINATING ACTIVITY (Corporate author)

Naval Postgraduate School
Monterey, California 93940

2a. REPORT SECURITY CLASSIFICATION

Unclassified

2b. GROUP

3 REPORT TITLE

THE ACTIVE COUPLING OF ELECTROMAGNETIC WAVES HAVING DIFFERING PHASE CONSTANTS

4. DESCRIPTIVE NOTES (Type of report and, inclusive dates)

Master's Thesis; December 1971

5. AUTHOR(S) (First name, middle initial, last name)

Albert Edward Whitehead; Lieutenant, United States Navy

6. REPORT DATE	7a. TOTAL NO. OF PAGES	7b. NO. OF REFS
December 1971	48	8

8a. CONTRACT OR GRANT NO.	9a. ORIGINATOR'S REPORT NUMBER(S)
b. PROJECT NO.	
c.	9b. OTHER REPORT NO(S) (Any other numbers that may be assigned this report)
d.	

10. DISTRIBUTION STATEMENT

Approved for public release; distribution unlimited.

11. SUPPLEMENTARY NOTES	12. SPONSORING MILITARY ACTIVITY
	Naval Postgraduate School Monterey, California 93940

13. ABSTRACT

The theory of active coupling of two waves with differing phase constants is examined. Experimental results supporting this theory are presented which include coupled power measurements and variations in coupling parameters as a function of the physical structure.

It is pointed out that this investigation could be applied directly to filter design and provides background work for the design of a broadband coupler.

DD FORM 1 NOV 65 1473 (PAGE 1)

S/N 0101-807-6811

UNCLASSIFIED

Security Classification

A-31408

KEY WORDS	LINK A		LINK B		LINK C	
	ROLE	WT	ROLE	WT	ROLE	WT
COUPLED MODE PROPAGATION						

133835

Thesis
W55544
c.1

Whitehead
The active coupling
of electromagentic
waves having differing
phase constants.